Renewable Energy 163 (2021) 123–137

Contents lists available at ScienceDirect

Renewable Energy

journal homepage: www.elsevier.com/locate/renene

Analysis on dynamic interaction between flexible bodies of large-sized wind turbine and its response to random wind loads

Shuangxi Guo [a, c, d, 1], Yilun Li [b, 1], Weimin Chen [a, d, *]

[a] Key Laboratory of Mechanics in Fluid Solid Coupling System, Institute of Mechanics, Chinese Academy of Sciences, Beijing, 100190, China
[b] Lab. MSSMat, CentraleSupélec, Université de Paris-Saclay, Gif sur Yvette, 91190, France
[c] AVIC Manufacturing Technology Institute, AVIC Composite Technology Center, Beijing, 101300, China
[d] School of Engineering Science, University of Chinese Academy of Sciences, Beijing, 100049, China

A R T I C L E   I N F O

Article history:
Received 4 March 2019
Received in revised form
5 August 2020
Accepted 24 August 2020
Available online 25 August 2020

Keywords:
Wind turbine
Dynamic response
Finite element simulation
Coupling system
Random wind loads

A B S T R A C T

Analysis of structural dynamic response of wind turbine is one of important issues to assess its structural integrity and safety during operation process. As the output power of wind turbine increasingly gets larger, the structural flexibility of the elastic components, such as rotor blades and supporting tower, of wind turbine gets larger owing to larger structural size, and, consequently, the dynamic interaction between these flexible bodies become more profound or, even, may have a significant impact on the dynamic response of the wind turbine. In this study, the integrated finite element model of a 5-MW wind turbine is developed so as to carry out dynamic response analysis, in terms of both time history and frequency spectrum, of the large wind turbine including multiple elastic bodies and their dynamic interactions. In order to have a deeper insight into the impact and mechanism of the dynamic interaction, the load transmission along its transmitting route and mechanical energy distribution during dynamic response under random wind loads are studied. And, the influences of the stiffness and motion of the supporting tower on the integrated system response are discussed.

Our numerical results show that the dynamic interaction between the elastic bodies may be significant during dynamic response. The response of the tower top becomes around 15% larger than that of the simplified model mainly due to the elastic deformation and dynamic vibration (called inertial-elastic effect) of the flexible blade; On the other hand, the elastic deformation may additionally consume around 10% energy (called energy-consuming effect) coming from external wind load, and, consequently, it could decrease the displacement of the tower. Therefore, there is a competition between the energy-consuming effect and inertial-elastic effect of the flexible blade on the overall dynamic response of the wind turbine. As for the blade response, the displacement of the blades gets up to 20% larger than that without blade-tower interaction, because the elastic-dynamic behaviors of the tower principally provides a more flexible and vibrating supporting base, which can significantly change the natural mode shape of the integrated wind turbine and can decrease the natural frequency of the blade.

1. Introduction

Wind turbine is essentially an integrated system composes of multiple flexible bodies such as slender blades, tube tower and its supporting part, which may introduce elastic structural deformation, vibration and then static/dynamic interaction between these flexible bodies during the operation process and dynamic response under external wind load. For example, under action of wind load along with rotation motion of rotor, blade is likely to elastically deform and vibrate, and this vibration can propagate and develop upon bottom tower through the rotation axis of hub, which introduces additional structure stress and, even, changes the rotor's spatial position on the tower top. Then the distribution of rotor aerodynamic force may change consequently, and the deformation and vibration of the blades could change too in return. As the electricity power increasingly rises, the structural size gets larger too, e.g. up to a level of, or more than, 100 m of tower height and/or rotor diameter. Consequently, the structural elasticity of blade and tower becomes more profound, and the interaction between the flexible bodies can no longer be neglected anymore. It is found that

* Corresponding author. Key Laboratory of Mechanics in Fluid Solid Coupling System, Institute of Mechanics, Chinese Academy of Sciences, Beijing, 100190, China.
E-mail address: wmchen@imech.ac.cn (W. Chen).
[1] These authors contributed equally to this work.

https://doi.org/10.1016/j.renene.2020.08.126
0960-1481/

tower elasticity can significantly influence the top blade deformation [1], and the shear stress caused by blade vibration can increase the tower displacement, even up to 300% [2]. Therefore, it becomes necessary to consider structural elasticity and dynamic coupling effect of flexible bodies for sake of an accurate and reliable strength/safety assessment during wind turbine operation process and dynamic response under wind loads.

Many models, mostly simplified, were used to analyze wind turbine strength and dynamic response, e.g., a single tower was considered, where other parts such as blade and nacelle are simplified as a centered mass, to calculate dynamic characteristics, or similarly a blade-only model was considered. Adhikari [3] regarded the top rotor as a centered mass on the tower top and calculated the frequency and response of the tower. By using similar model, Negm [4] optimized the structural properties of a tower, and Bazeos [5] studied the static strength and anti-seismic performance of a steel tower. These researches provided fundamental results for wind turbine design in practice, while it is noted that the structural coupling effect of those flexible bodies is somewhat simplified, or not included, there.

In recent years, in order to consider a multi-body-coupling wind turbine, some researchers studied a single tower (or blade) by ways of introducing proper boundary conditions, which is used to model the action coming from other parts of the integrated wind turbine. Murtagh [6] considered the shear force coming from the turbine blades as a coupling force acted on the tower top during solving the tower dynamic equations to analyze the coupling of blade and tower. He further presented the influence of harmonic mass-damper on wind turbine vibration [7]. Similarly, Chen [2] examined the coupling effects, through the wind load and the tower response analysis, he pointed out that if the blade shear force was included the tower displacement would increase by up to 2 times. Spagnoli [8] presented the dynamic response of two wind turbines and compared his results with that under static-uniform pressure. Based on dynamic equations of a one-degree of freedom tower and a flexible blade, Liu [9] presented the natural frequencies of the blade-tower model. He lumped the top turbine as a concentrated mass, then he gave the wind loads under consideration of tower first bending mode.

Further, some other researchers developed a mixed model which combines rigid body and flexible body together, where the dynamic-flexible-behavior of other parts was considered as a unidirectional effect instead of coupling effect. Lee [10] used the Floquet theory to solve out the eigenvalue of a rigid-flexible-body through assuming the linear combination of steady solutions. He gave out the frequency and modal shape of a two-blade wind turbine while the dynamic response was still unknown. Wang [1] also theoretically solved the multi-body equations, and he pointed out the tower stiffness can significantly change the blade displacement. Kang [11] developed a coupled equation group of a blade-tower model to study the stability of wind turbine, and he found that at a certain mixed natural mode of blade-tower system it may be unstable. Shkara [12] considered the blade-tower aerodynamic coupling, he used CFD and coupled model to predict the aerodynamic loads acting on the tower due to the vortex shedding from the front blades. Using the nonlinear vortex correction method, Kim [13] studied the influence of aero-elastic coupling on the aerodynamic loads acting on upwind wind turbine. Still, the coupling mechanism between different flexible bodies of the wind turbine system needs a further study.

In this study, the dynamic response, in terms of both time history and frequency spectrum, of a large-sized wind turbine is presented, based on our finite element model of the integrated blade-tower system. Here we can consider the elastic deformation and dynamic interactions of the flexible bodies, such as the blade and tower. In order to have a deeper insight into the mechanism and impact of the elastically dynamic interaction, the load transmission along its transmitting route and the mechanical energy distribution during the whole dynamic response under random wind loads are studied and compared, i.e. for cases of three different models. At last, the influences of the stiffness and motion of the supporting tower on the overall integrated system response are discussed, from the view of the supporting base properties through the theoretical analysis.

2. Integrated wind turbine models and natural dynamic characteristics

2.1. Dynamic governing equations of coupled wind turbine system

As the main flexible parts of a wind turbine shown in Fig. 1, both the tower and blade can be assumed as Euler beams because their axial dimensions are much larger than the lateral dimensions. It is noted that the structural properties, i.e. the mass and stiffness, are axially variable since the cross-sections of the blade/tower change along the structural axial direction. Additionally, the body forces, including the gravity F_{gra} of blade/nacelle/tower and the centrifugal force F_{cen} owing to blade rotation, are considered here. For the blades of wind turbine, their centrifugal force may introduce an effect of stiffness strengthening. Guo [14] and Li [15] studied this effect by using the FEM (finite element method) and Kane method. They found that it can increase the natural frequencies (e.g. by 7%) and decrease the dynamic response. And, the structural gravity may change the blade's response at different azimuth, e.g. by around 15% [14].

The governing equations of the dynamics of the tower/blade, regarded as Euler beam, are expressed as

$$
\begin{aligned}
&m(\xi_B)\frac{\partial^2 w(\xi_B,t)}{\partial t^2}-\frac{\partial}{\partial \xi_B}\left(T(\xi_B)\frac{\partial w(\xi_B,t)}{\partial \xi_B}\right)+\frac{\partial^2}{\partial \xi_B^2}\left(EI(\xi_B)\frac{\partial^2 w(\xi_B,t)}{\partial \xi_B^2}\right)=F(\xi_B)\\
&m(\xi_T)\frac{\partial^2 w(X,t)}{\partial t^2}-\frac{\partial}{\partial \xi_T}\left(T(\xi_T)\frac{\partial w(\xi_T,t)}{\partial \xi_T}\right)+\frac{\partial^2}{\partial \xi_T^2}\left(EI(\xi_T)\frac{\partial^2 w(\xi_T,t)}{\partial \xi_T^2}\right)=F(\xi_T)
\end{aligned}
\tag{1}
$$

where $w(\xi,t)$ is the transverse displacement, and ξ_T and ξ_B is generalized coordinates represents the axial location of the tower and blade in their local coordinate system. $m(\xi)$ is the mass per unit length, t is the time. $T(\xi)$ is the axial force caused by gravity/centrifugal force, and $EI(\xi)$ is the bending stiffness. $F(\xi)$ is the external load coming from wind load or the wind load transmitted through the blade to the tower.

For the tower, its bottom is fixed on the ground, and the nacelle with the rotating blade is located at its top. If considering the tower

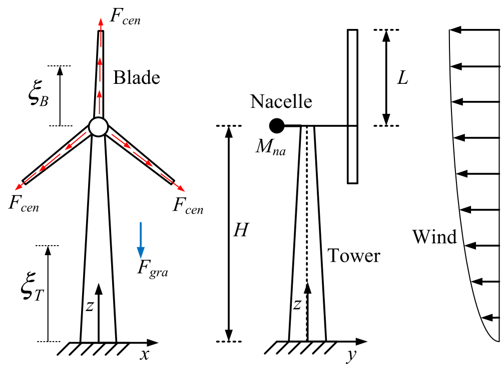

Fig. 1. Schematic of a coupled wind turbine system.

separately, the boundary conditions for the tower can be divided into displacement boundary conditions and load boundary conditions. At the tower bottom, both the displacement and the curvature are zero, i.e.

$$w(\xi_T,t)|_{\xi_T=0}=0 \quad \left.\frac{\partial w(\xi_T,t)}{\partial \xi_T}\right|_{\xi_T=0}=0 \tag{2}$$

At the tower top, it is noted that the tower top subjects to not only the wind load and also the coupling forces, due to dynamic motion and elastic deformation of blades and nacelle, during dynamic response to wind loads. Thus, the bending moment is equal to the moment caused by the gravity of nacelle and blade, and the shear force comes from the motion of the nacelle and the blades. We have

$$\begin{aligned} &\left.EI(\xi_T)\frac{\partial^2 w(\xi_T,t)}{\partial \xi_T^2}\right|_{\xi_T=H}=Q \\ &\left.\frac{\partial}{\partial \xi_T}\left(EI(\xi_T)\frac{\partial^2 w(\xi_T,t)}{\partial \xi_T^2}\right)\right|_{\xi_T=H}=(M_{na}+3M_B)\left.\frac{\partial^2 w(\xi_T,t)}{\partial t^2}\right|_{\xi_T=H}+\sum_{i=1}^{3}\int_0^L m^i(\xi_B)\frac{\partial^2 w^i(\xi_B,t)}{\partial t^2}d\xi_B \end{aligned} \tag{3}$$

where H is the height of the tower, Q is the bending moment caused by the gravity of nacelle and blade. M_{na} is the mass of the nacelle, M_B is the total mass of one blade.

If considering the blade separately, it can be regarded as a cantilever beam of which root is fixed on the top of the tower. It is also noted that the blade's load conditions should include not only the external wind load and also the forces coming from the supporting tower, due to motion and elastic deformation of the flexible tower. So boundary conditions of the blade are like this: at the free end of the blade, both the shear force and the moment are zero

$$\begin{aligned} &\left.EI(\xi_B)\frac{\partial^2 w(\xi_B,t)}{\partial \xi_B^2}\right|_{\xi_B=L}=0 \\ &\left.\frac{\partial}{\partial \xi_B}\left(EI(\xi_B)\frac{\partial^2 w(\xi_B,t)}{\partial \xi_B^2}\right)\right|_{\xi_B=L}=0 \end{aligned} \tag{4}$$

where L is the length of the blade. And at the root end of the blade, the continuous condition should be considered, i.e. the displacement and the curvature of the blade are consistent with that of the tower top as follows

$$w(\xi_B,t)|_{\xi_B=0}=w(\xi_T,t)\Big|_{\xi_T=H} \text{ and } \left.\frac{\partial w(\xi_B,t)}{\partial \xi_B}\right|_{\xi_B=0}=\left.\frac{\partial w(\xi_T,t)}{\partial \xi_T}\right|_{\xi_T=H} \tag{5}$$

As for the nacelle, given that the stiffness of the nacelle is much larger than the blade and tower, the nacelle is assumed to be a point mass attached to the top of the tower. So the equation of the nacelle motion is

$$M_{na}\ddot{w}_{na}=F_{na} \tag{6}$$

where w_{na} is the displacement of the nacelle and F_{na} is the overall force acted on the nacelle. The displacement of the nacelle is the same with the top of the tower and the force F_{na} is balanced with the shear force at the top of the tower and the root of the blades

$$\begin{aligned} &w_{na}(t)=w(\xi_T,t)|_{\xi_T=H} \\ &F_{na}+\sum_{i=1}^{3}EI^i(\xi_B)\left.\frac{\partial^2 w^i(\xi_B,t)}{\partial \xi_B^2}\right|_{\xi_B=0}+EI(\xi_T)\left.\frac{\partial^2 w(\xi_T,t)}{\partial \xi_T^2}\right|_{\xi_T=H}=0 \end{aligned} \tag{7}$$

By solving equations (1) and (6) and using the boundary conditions equations (2)–(5) and (7), we can get the response of the integrated wind turbine system. Here numerical simulations based on FEM are used to get the dynamic response of the integrated wind turbine under random wind load. And the interactions between the flexible bodies, i.e. the blades and tower, during the dynamic responses are examined.

2.2. The FEM models

To examine the impact of the flexible-body interaction on dynamic response, we built three FEM models as shown in Fig. 2, i.e. Model 1, the integrated wind turbine model including three flexible blades and a tower on the top of which the hub and nacelle are simplified as lumped mass; Model 2, the simplified flexible tower-only model where the other parts like the blades, hub and nacelle are simplified as lumped masses, and the tower bottom end is fixed; Model 3, the simplified blade-only model of which roots are fixed on the top of the rigid tower as a cantilever beam. In our FEM models, every blade was uniformly divided into 123 Euler beam elements, and the tower was divided into 100 beam elements. The tower is fixed at the bottom end.

For the integrated system including the blades and nacelle and tower, the dynamic equation indicates the balance of the forces including the structural inertial and damping forces and the environmental load (wind forces). It can be written as

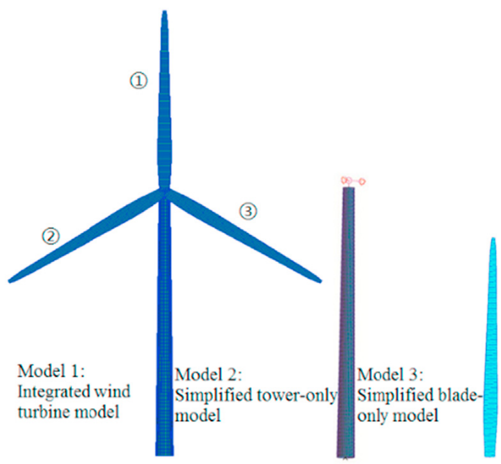

Fig. 2. Integrated wind turbine model, along with the simplified tower-only and blade-only models.

$$\begin{bmatrix} M_B & M_{12} & M_{13} \\ M_{21} & M_{na} & M_{23} \\ M_{31} & M_{32} & M_T \end{bmatrix} \begin{bmatrix} \ddot{U}_B \\ \ddot{U}_{na} \\ \ddot{U}_T \end{bmatrix} + \begin{bmatrix} C_{11} & C_{12} & C_{13} \\ C_{21} & C_{22} & C_{23} \\ C_{31} & C_{32} & C_{33} \end{bmatrix} \times \begin{bmatrix} \dot{U}_B \\ \dot{U}_{na} \\ \dot{U}_T \end{bmatrix} + \begin{bmatrix} K_{11} & K_{12} & K_{13} \\ K_{21} & K_{22} & K_{23} \\ K_{31} & K_{32} & K_{33} \end{bmatrix} \begin{bmatrix} U_B \\ U_{na} \\ U_T \end{bmatrix} = \begin{bmatrix} F_B \\ F_{na} \\ F_T \end{bmatrix} \tag{8}$$

where U_B is the displacement vector of the blades, U_{na} and U_T are respectively the displacement vectors of the rigid nacelle and the tower. And M_{ij}, C_{ij}, K_{ij} are the mass matrix, damping matrix and stiffness matrix respectively. The right side term, the system force, essentially involves the environmental loads (wind forces), structural body forces (gravity force and centrifugal force of rotating blade) and the inertia force, and these forces are acted on various parts of the wind turbine and respectively involved into the three force sub-vectors, F_B, F_{na} and F_T. It is noted that the non-diagonal elements of the system matrices imply the mass/stiffness/damping interactions between different bodies.

The load conditions of beam element used here include the axial force, and the moments of bending, in *oxz* and *oxy* two planes, see Fig. 3 where a beam element and the local *xyz* coordinate system are shown. ρ is the structural mass density, and l is the length of the beam element. E is the Young's modulus. $\boldsymbol{I_z}$ is the inertial moment around the neutral axial paralleling to the axis z, and $\boldsymbol{I_y}$ is the inertial moment around the neutral axial paralleling to the axis y. If the two nodes of the beam element are numbered as i and i+1, the displacement vector of the element is written as

$$u^e = \left[u_i, v_i, w_i, \theta_{xi}, \theta_{yi}, \theta_{zi}, u_{i+1}, v_{i+1}, w_{i+1}, \theta_{xi+1}, \theta_{yi+1}, \theta_{zi+1}\right]^T \tag{9}$$

The corresponding load vector of the element is

$$P^e = \left[P_{xi}, P_{yi}, P_{zi}, M_{xi}, M_{yi}, M_{zi}, P_{xi+1}, P_{yi+1}, P_{zi+1}, M_{xi+1}, M_{yi+1}, M_{zi+1}\right]^T \tag{10}$$

where $\boldsymbol{u_i}$ is the axial displacement, and $\boldsymbol{v_i}$ and $\boldsymbol{w_i}$ are the transverse displacements. θ_i is the rotational angle. For the tower and blades, the rotational displacement can be neglected here. Then the vectors of displacement and load are rewritten as

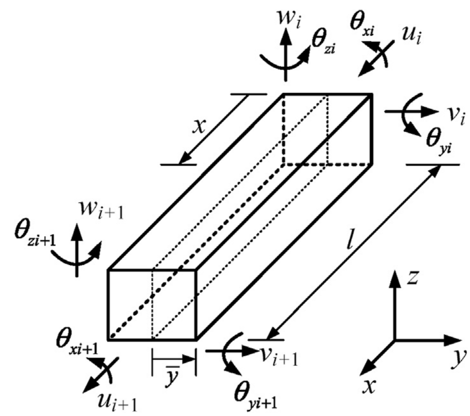

Fig. 3. Beam element in the local coordinate system.

$$\begin{aligned} u^e &= \left[u_i, v_i, w_i, \theta_{yi}, \theta_{zi}, u_{i+1}, v_{i+1}, w_{i+1}, \theta_{yi+1}, \theta_{zi+1}\right]^T \\ P^e &= \left[P_{xi}, P_{yi}, P_{zi}, M_{yi}, M_{zi}, P_{xi+1}, P_{yi+1}, P_{zi+1}, M_{yi+1}, M_{zi+1}\right]^T \end{aligned} \tag{11}$$

where P^e is the load vector of each element, M_i is the moment acting on the element. According to Eq. (11), the displacement can be divided into three parts, i.e. the axial displacement along the x direction and the displacements respectively in the planes *oxy* and *oxz*. And the corresponding element stiffness matrix can be obtained as follows. In case that the cross-section size of the tower and blade changes with axial location, in the FEM model the element number is enough to guarantee that the change of the cross-section dimension is small in an arbitrary element, so each element can be treated as a beam with constant cross-section, and the constant cross-section area is equal to the mean of the cross-sectional area at both ends.

A) The axial displacement along the x direction

In the local coordinate system *oxy*, the axial displacement vector is $u_x^e = [u_i, u_{i+1}]^T$, the corresponding load vector of the element is $P_x^e = [P_{xi}, P_{xi+1}]^T$. The displacement field of the element is

$$u(x) = u_i + \left(\frac{u_{i+1} - u_i}{l}\right)x = \left(1 - \frac{x}{l}\right)u_i + \frac{x}{l}u_{i+1} = N_x(x)u_x^e \tag{12}$$

where the displacement function is assumed as $N_x(x) = [1 - x/l, x/l]$. And the element matrix of stiffness and mass (centered mass) can be written as

$$K_x^e = EAl \times B^T \times B = \frac{EA}{l}\begin{bmatrix} 1 & -1 \\ -1 & 1 \end{bmatrix} \quad and \quad M_x^e = \frac{\rho Al}{2}\begin{bmatrix} 1 & 0 \\ 0 & 1 \end{bmatrix} \tag{13}$$

where the strain matrix is $B_x(x) = dN_x(x)/dx = [-1/l, 1/l]$, A is the area of cross section. The governing equation of the element is

$$M_x^e \ddot{u}_x^e + K_x^e u_x^e = P_x^e \tag{14}$$

where the axial force P_x^e includes the axial force F_{cen}^e and F_{gra}^e that represent the gravity force and centrifugal force acted on each element.

B) The displacement in plane *oxy*

If the pure bending in plane *oxy* is only considered, displacement vector of point i includes v_i and θ_{zi}, i.e. the displacement v_i along y direction and rotation angle θ_{zi} around axis z. The element displacement vector and the corresponding load vector are $u_y^e = [v_i, \theta_{zi}, v_{i+1}, \theta_{zi+1}]^T$ and $P^e = [P_{yi}, M_{zi}, P_{yi+1}, M_{zi+1}]^T$. The displacement field of the beam element is assume as a polynomial function of the third order

$$u_y^e = a_0 + a_1 x + a_2 x^2 + a_3 x^3 \tag{15}$$

where a_0, a_1, a_2 and a_3 are four undetermined coefficients. According to the node displacement u_y^e, the displacement function can be written as

$$\begin{aligned} v(x) = &\left(1 - 3\xi^2 + 2\xi^3\right) v_i + l\left(\xi - 2\xi^2 + \xi^3\right)\theta_{zi} \\ &+ \left(3\xi^2 - 2\xi^3\right) v_{i+1} + l\left(\xi^3 - \xi^2\right)\theta_{zi+1} = N_y(x) u_y^e \end{aligned} \tag{16}$$

where $\xi = x/l$, and the element matrix of displacement function $N_y(x)$ is

$$N_y(x) = \left[1 - 3\xi^2 + 2\xi^3, l\left(\xi - 2\xi^2 + \xi^3\right), 3\xi^2 - 2\xi^3, l\left(\xi^3 - \xi^2\right)\right] \tag{17}$$

Now the element matrix of stiffness and mass can be written as:

$$K_y^e = \int_0^l \int_A B_y^T E B_y dA dx = \frac{EI_z}{l^3} \begin{bmatrix} 12 & 6l & -12 & 6l \\ 6l & 4l^2 & -6l & 2l^2 \\ -12 & -6l & 12 & -6l \\ 6l & 2l^2 & -6l & 4l^2 \end{bmatrix} \quad and \quad M_y^e = \frac{\rho A l}{2} \begin{bmatrix} 1 & 0 & 0 & 0 \\ 0 & 0 & 0 & 0 \\ 0 & 0 & 1 & 0 \\ 0 & 0 & 0 & 0 \end{bmatrix} \tag{18}$$

where the strain matrix is $B_y(\xi) = -\bar{y}(d^2 N_y(x)/dx^2) = -2\bar{y}[(6\xi - 3)/l^2, (3\xi - 2)/l, -(6\xi - 3)/l^2, (3\xi - 1)/l]$,$\bar{y}$ is the distance from the point to the neutral axis. The governing equation of the element is

$$M_y^e \ddot{u}_y^e + K_y^e u_y^e = P_y^e \tag{19}$$

Similarly, for case of the pure bending in plane oxz, the element matrix of stiffness and mass can be obtained. Combining Eq.s (14) and (19) can yield the element equations, and by assembling the element equations we have the governing equations of the beam with axially-variable stiffness/mass.

As for the nacelle on the tower top, its stiffness is much larger than the flexible blades and tower, so it can be regarded as a centered mass point fixed at the tower top. In that case the governing equation of the dynamics is simply written as

$$\begin{bmatrix} M_{na} & 0 & 0 \\ 0 & M_{na} & 0 \\ 0 & 0 & M_{na} \end{bmatrix} \begin{bmatrix} \ddot{u}_{nax} \\ \ddot{u}_{nay} \\ \ddot{u}_{naz} \end{bmatrix} = \begin{bmatrix} F_{nax} \\ F_{nay} \\ F_{naz} \end{bmatrix} \tag{20}$$

And, the three-dimension compatible elements are used to connect the rigid body and flexible body in our FEM model so that the calculation process would not be singular during the whole dynamic response.

To run the dynamic response analysis, a numerical simulation is used to solve the FEM dynamic equations. Among those direct numerical integration methods like the Newmark and the Finite Difference methods, the Newmark method is employed here so as to adjust the distribution of the structural acceleration during the integration range by properly changing the integration parameters. The interpolation functions of the displacement and acceleration are written as

$$\begin{aligned} \dot{U}_{t+\Delta t} &= \dot{U}_t + [(1-\beta)\ddot{U}_t + \beta \ddot{U}_{t+\Delta t}]\Delta t \\ U_{t+\Delta t} &= U_t + \dot{U}_t \Delta t + \left[\left(\frac{1}{2} - \alpha\right)\ddot{U}_t + \alpha \ddot{U}_{t+\Delta t}\right]\Delta t^2 \end{aligned} \tag{21}$$

where the values of α and β are respectively 1/6 and 1/2 at every time step during the dynamic response.

2.3. Natural dynamic characteristics of the integrated wind turbine

The structure parameters are based on the 5-MW wind turbine developed by the NREL (National Renewable Energy Laboratory) of the United States. The tube tower height is 87.6 m. The values of the diameter and thickness of the tower linearly changing from the bottom, i.e. 6 m and 35.1 mm, to the top, i.e. 3.87 m and 24.7 mm [16], respectively. And other geometrical and material parameters are listed in Table 1, where the blade's parameters are given according to LMH64-5 [17], and the structural damping is 0.01 [16].

Structure vibration often happens under operation conditions that various environmental loads and body forces such as dynamic wind load, structural gravity force and rotor's centrifugal force may significantly act on the whole wind turbine. Particularly, when the frequency of the external load is coincident with the structural frequency, resonance with large amplitude will happen, which may induce structure fatigue life and, even, directly result in body damage. So the analysis of natural dynamic characteristics is the basic design work so that the structural natural frequency is different from the external load as far as possible to avoid harmful resonance. Here we calculate the natural frequencies of the wind turbine including both flexible blades and tower and compared the results with that given by Jonkman [16], and, moreover, the frequencies of the first three along-wind tower bending modes(the

Table 1
Main parameters of the wind turbine.

Parameters	Value	Parameters	Value
Blade number	3	Tower mass density	8 500 kg/m^3
Rotor, Hub Diameter	126 m, 3 m	Tower elastic modules	210 GPa
Hub height	90 m	Tower shear modules	80.8 GPa
Rated wind speed	11.4 m/s,	Blade length	61.5 m
Rated rotor speed	12.1r/min	Blade elastic modules	14.8 GPa
Rotor whole mass	110 000 kg	Blade mass density	1 700 kg/m^3
Nacelle whole mass	240 000 kg		

mode 1,5 and 6) are compared with the simplified tower model in Table 2. Satisfied agreement between our numerical and Jonkman's results, i.e. less than 5% difference, is seen.

Except the first bending frequency of the blade-tower model is a little smaller than the tower-only model, the frequencies of modes with higher order number are slightly larger than the simplified model. The reason might be that for the first bending mode, the top blade deformation plus the bottom tower deformation makes up the modal shape, as if the length of a beam gets larger, so the overall flexibility is smaller than the case of tower-only. While for the higher-order bending modes, the modal shapes become more complicated and higher-order deformation of the blades may increase the modal stiffness of the blade-tower system, which could increase the modal frequency.

Additionally, some selected modal shapes are presented in Fig. 4. It is noted that the modal shapes of the blade-tower model are somewhat different from those simplified models. Compared to either the tower-only model or the blade-only model, there are some additional and/or different modes. For examples, the rotor mode in Fig. 4b presents a leading-lag-still modal shape which does not occur to the simplified blade model. And the blade flapping modes, either symmetric or anti-symmetric mode as shown in Fig. 4 e and f, show different modes compared to the blade-only model. What's more, we see some blade-tower-coupling modes, e.g. modes in Fig. 4a, b and c, where these coupling modal shapes actually indicate the interaction between the blade and tower deformations. So we may say, for the blade-tower-coupling system, its modal shapes are more complicated, and there are some additional and different modes that should be noted.

3. Dynamic responses under random wind loads

The dynamic responses, including the structural displacements and stresses of Model 1, are calculated under random wind loads and compared with the two simplified models, i.e. Model 2 and 3 respectively. Regarding the typical dynamic behavior of the rotor blade, the body forces, such as the centrifugal and gravity forces of the blades, are considered as distributing loads, which act along the

Table 2
Natural frequencies of different models.

Mode	Integrated Turbine/Hz	Simplified Turbine/Hz	Ref. [16]/Hz	Difference/%
1	0.311	0.315	0.320	2.9
2	0.659	/	0.630	4.4
3	0.689	/	0.669	2.9
4	0.722	/	0.702	2.8
5	2.819	2.712	/	/
6	7.279	7.198	/	/

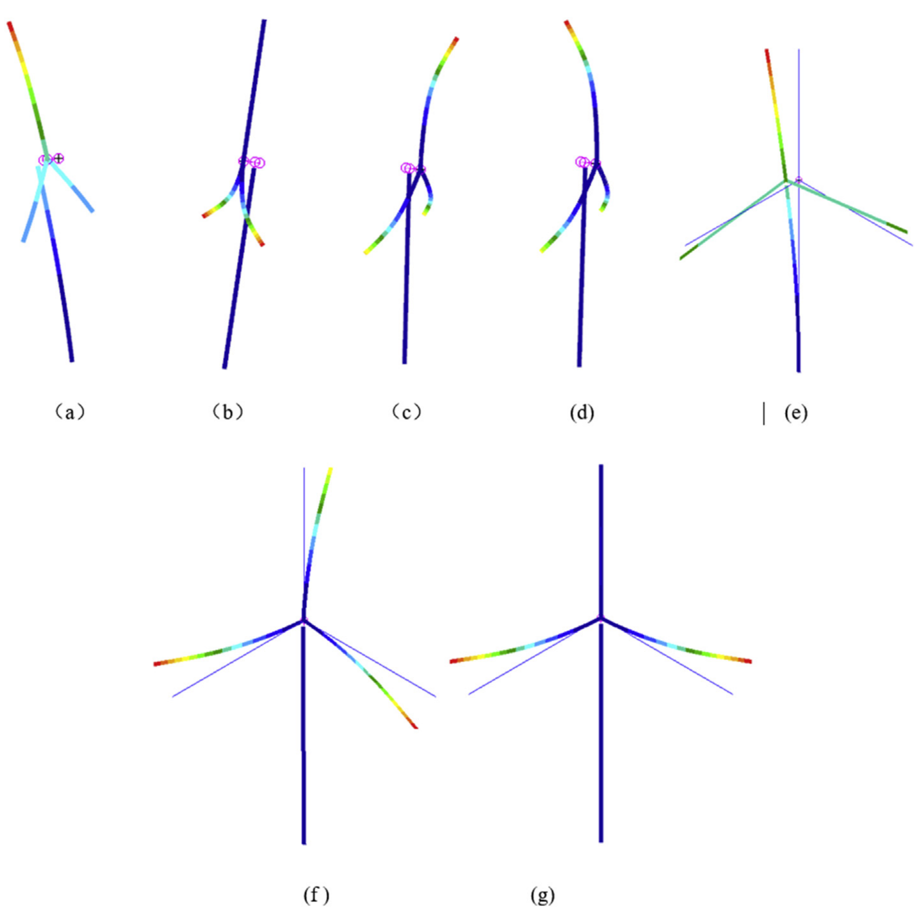

Fig. 4. Selected modal shapes of the integrated wind turbine.

blade span respectively in two directions so as to simulate the mechanical effects owing to rotor rotation. The wind load is uniformly acted on every single blade in the direction vertical to the rotor plan. As we know, in practice, the wind speed mostly shows randomness, and there essentially exists a temporal-spatial correlation of wind speed distribution. Then, among the popular wind spectrums such as Harris spectrum, Kaimal spectrum and DNV (Det Norske Veritas) and IEC61400 criteria, we choose the mostly used Kaimal spectrum [18] to give a time history approximation of wind speed and the consequent wind load. The wind speed spectrum is written as

$$PSD(f) = \frac{I^2 V_{10\min} l}{\left(1 + 1.5\frac{fl}{V_{10\min}}\right)^{5/3}} \tag{22}$$

where I is the turbulence intensity. $V_{10\min}$ is the averaged wind speed in 10 min at the given point. l is the scalar which has the values of $l = 20h$ when the height $h < 30m$ and $l = 600$ when $h \geq 30m$ respectively. f is the wind frequency. If we take the averaged wind speed as $V_{10\min} = 11.4$ m/s, $I = 0.1$ and the time step as 0.02s, the time history of wind speed at the tower top height (90 m) among 200s time duration is plotted in Fig. 5.

For a slender body, the drag force of the wind can be given by the empirical expression [6] as

$$F(t) = \frac{1}{2} C_D \rho_{air} A v^2(t) \tag{23}$$

where C_D is the drag coefficient, and the value is 2.0 here. ρ_{air} is the air density and has the value of 1.25 kg/m^3. A is the windward area of the blade, and $v(t)$ is the instant wind speed. Then the direction integration based on the Newmark method is used to solve out the dynamic response of the wind turbine, described in Eq. (8), under the wind load. The interactions between the flexible tower and blades during the dynamic response are examined in two ways, i.e. the impacts of elastic tower on the blade response and impacts of elastic blade on the tower response, in Section 3.1 and 3.2 respectively. Further, the mechanism of the interactions will be discussed in Section 4.

3.1. Influences of elastic tower on blade dynamic response

Essentially, the base supporting stiffness of a blade topped on the integrated model (Model 1 in Fig. 2) is different from the simplified blade-only model (Mode 3 in Fig. 2). Or, the practical blade is actually supported on the top of the flexible tower which

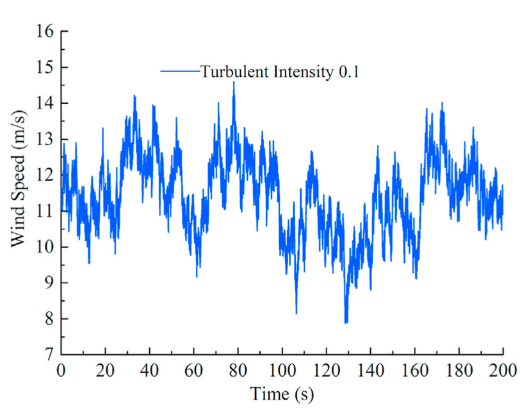

Fig. 5. Time history of the wind speed at the tower top (90 m).

may deform, vibrate and, even, interact with the top blade, while the simplified one is just ideally fixed at its root.

Selected displacements of the blade tip are presented and compared in Fig. 6, in terms of the spectrum curves, where blade 1 and blade 2 are considered, because the two blades represent different gravity effects owing to their different spatial positions, as shown in Fig. 2. Generally speaking, comparing the spectrum curves of these blades, the peak behaviors are quite different, in terms of the peak number, the amplitude and frequency values. For case of the integrated model, there are more response peaks which happen at those additional modal frequencies of the coupled system, such as the tower pitch and the higher-order coupled blade modes, compared to the simplified blade-only model.

Comparing Fig. 6a and b, we can see that the displacement amplitude of the integrated model gets larger by around 22%, or tower deformation and vibration may amplify the response of the blade at tower top. And, comparing Fig. 6b and d, it is seen that the displacement amplitudes of different blades obviously vary, mainly because the modal shapes of the two blades are different. It is also noted that the maximum amplitudes happen at different frequencies, i.e. at 0.311 Hz for blade 1 while at 0.677 Hz for blade 2. Because the frequency 0.311 Hz (or 0.677 Hz) corresponds to the natural mode that the blade has the maximum modal shape deformation. The time history of the blades' displacement is shown in Fig. 7.

Comparing the maximum bending stress of the three blades, listed in Table 3, it shows that the bending stress depends on the blade's azimuth (or the rotation position). More specifically, the root stress of blade 1 rises by 11.7% while blade 2 rises by only 1.2% respectively, compared to the blade-only model. That's in part because of the anti-symmetrical flapping modes of the integrated tower-blade model, which makes the dynamic behavior of blades at different positions change significantly.

3.2. Influences of elastic blades on the tower dynamic response

The spectrum of tower top displacements, presented in Fig. 8a, show that the peak value of the integrated model drops significantly, i.e. being nearly two-thirds of the tower-only model, while its peak locates at the frequency of tower first-bending. If concerning only the tower response of the first-bending mode, because the blade elastic deformation, actually accounting for a profound part of the overall system deformation, can consume a lot overall energy coming from the wind, the tower deformation consequently gets smaller. That could be further proved through a comparison of the time histories of tower-top displacement of the two models, as shown in Fig. 8b. The tower maximum bending stress of the integrated model remarkably drops to 15.3 MPa, comapred with 20.5 MPa of the simplified model. That is to say the tower stress may be overestimated if using the simplified model, by up to 25.4%.

4. Discussions on coupling mechanism between elastic blade and tower during dynamic response

Comparing the two displacement spectrums of the tower top, plotted in Fig. 9, it is noted that if the dynamic interaction between the elastic blades and tower is involved, not only the peak value of the displacement amplitude changes, but also the peak frequency (at which the displacement approaches its peak) changes. More specifically, the peak displacement gets larger while the peak frequency gets smaller. And it is also noted that the random wind load essentially changes with its frequency, in some way irregularly as shown in Fig. 9c, owing to its dependence on the phase angle and the nonlinear relationship between wind load and velocity, as shown in Eq. (23). So we may say that there are mainly two reasons

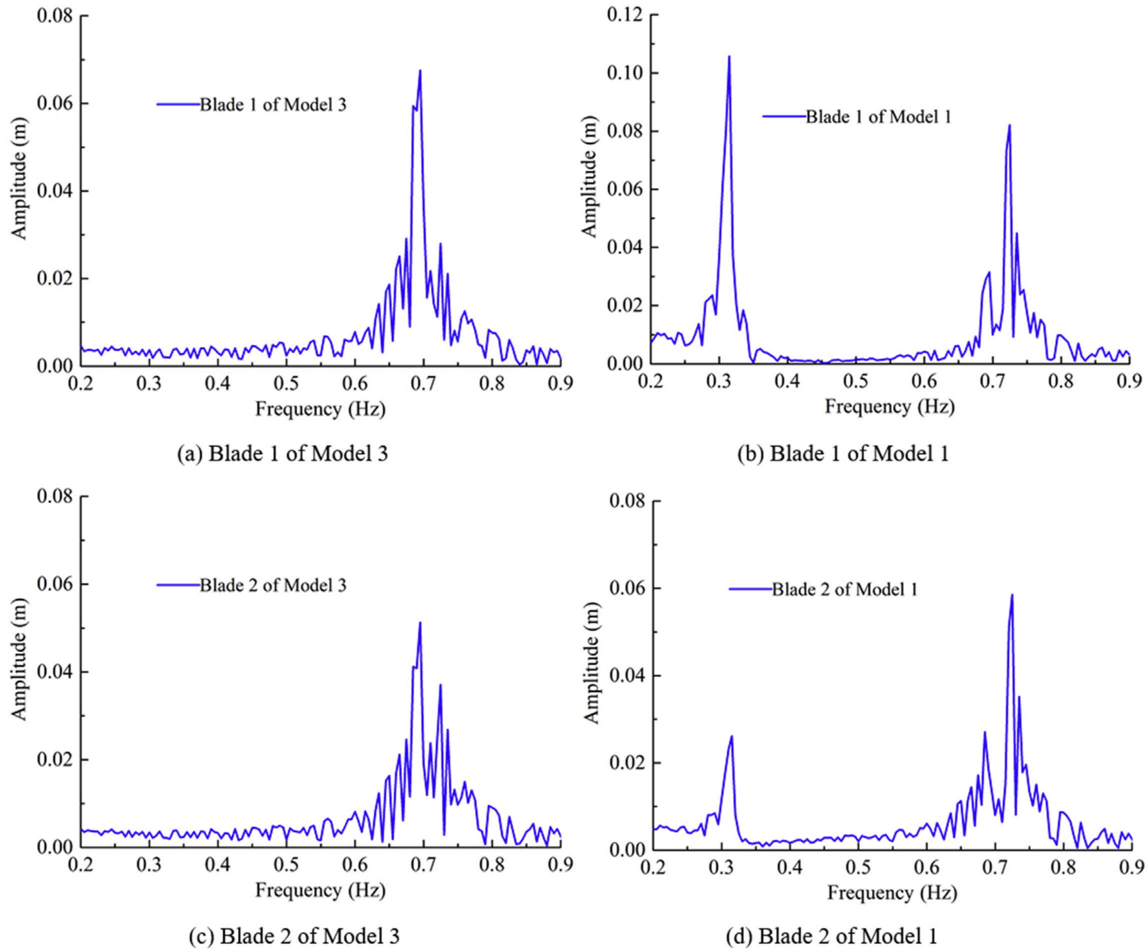

Fig. 6. Displacement frequency spectrums for the blades using different FEM models.

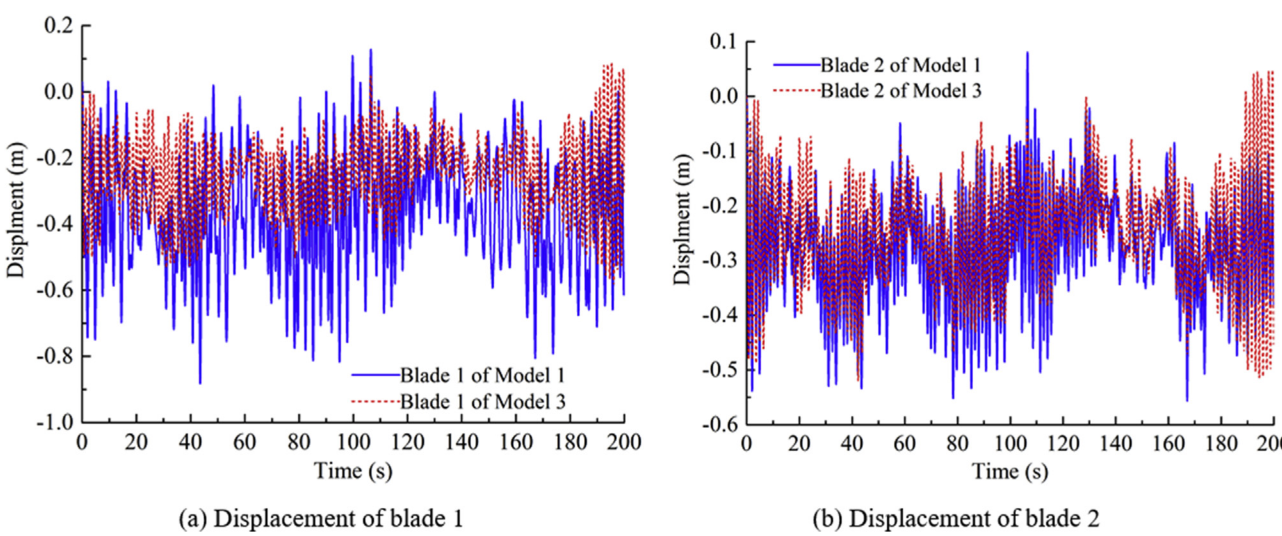

Fig. 7. Time history of the blades' displacement.

Table 3
Maximum stress of the blades.

Component	Stress/MPa	Component	Stress/MPa
Blade 1 of model 3	6.88	Blade 2 of model 3	6.73
Blade 1 of model 1	7.69	Blade 2 of model 1	6.81

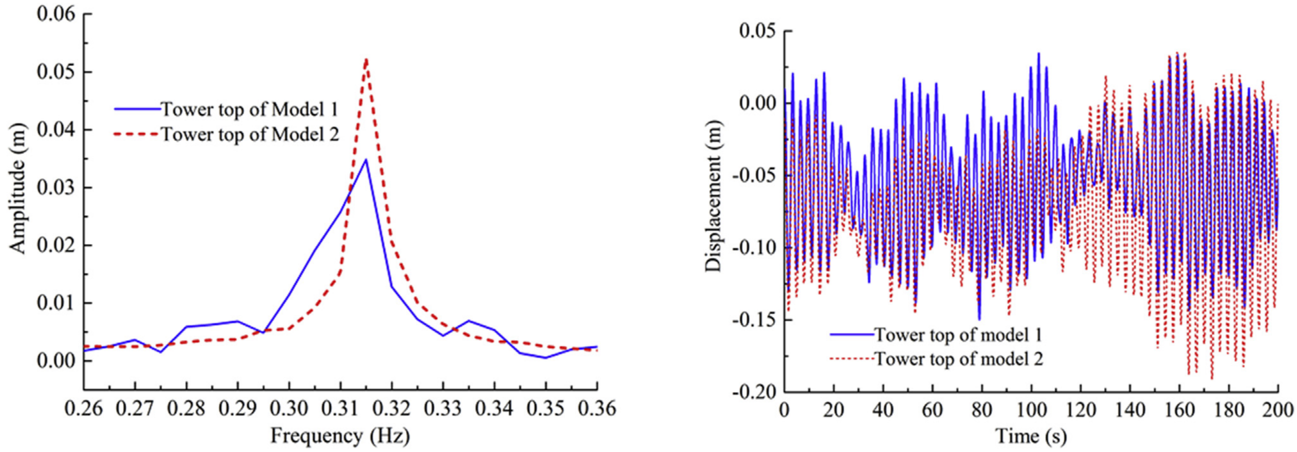

(a) Frequency spectrum (b) Time history

Fig. 8. Displacement response of the tower top.

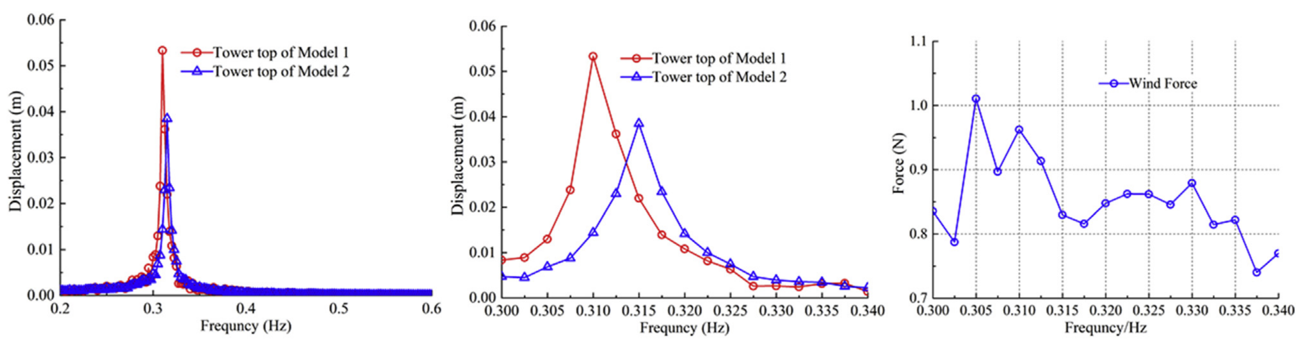

(a) Spectrum of tower displacement (b) Spectrum at the tower bending frequency (c) Spectrum of the wind load

Fig. 9. Frequency spectrum of the tower top response.

which are responsible for the response differences, i.e. one is the structural dynamic coupling between flexible bodies and another one is the different values of the wind load at different frequencies. And, the effect of structural dynamic coupling between flexible bodies, i.e. the impact of flexible blades on tower response and the increase of blade displacement caused by elastic tower, will be discussed in details through frequency response analysis.

4.1. Tower response increase caused by top Blade's flexible and inertial behaviors

In order to examine the impact of flexible blades on tower response, two wind load cases are considered, i.e. in Case 1 the wind load is uniformly distributed on the three blades and in Case 2 the wind load, as a concentrated force *F*, is acted directly on the tower top, see Fig. 10. And, the response of the simplified tower-only model (Case 3) is given as a comparison so as to have a deeper insight into the blade-tower coupling mechanism.

The displacement spectrum curves of the tower top, ranging from 0.0 Hz to 3.0 Hz, and the spectrum of load at the tower top are presented in Fig. 11. It shows that the maximum displacement amplitude happens at the first-bending frequency. Particularly, the local spectrum, ranging from 0.28 Hz to 0.34 Hz, is presented in Fig. 11b. It is seen that the displacement amplitude rises by 15.0% and the bending frequency drops a little compared with the simplified tower-only model. Principally because, for the integrated blade-tower model, its overall structural length and, therefore,

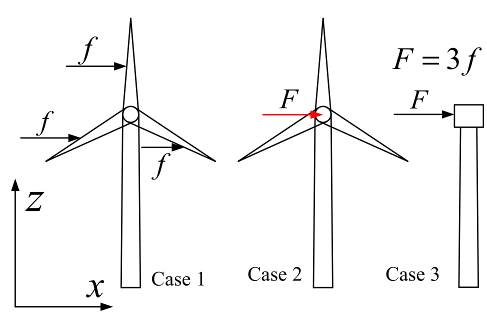

Fig. 10. Three Cases considering various wind loads, acting on the coupled and simplified models respectively.

bending flexibility get larger. Additionally, the wind load spectrum, presented in Fig. 11c, shows that the value of wind load at the first-bending frequency gets 14.0% larger than the simplified model. This wind load amplification can also be seen in the load spectrums for Cases 1 and 2, see Fig. 11d, where the wind load at the first-bending frequency gets 15.7% larger than the simplified model due to the effects coming from blade inertia and deformation.

To explain the reason why the wind load, running through the flexible blade to the tower top, becomes larger, here we take a one degree-of-freedom (DOF) system as an example (shown in Fig. 12a), for clarity and simplicity, to give its theoretical solution. The governing equation of the one-freedom-degree system can be written as

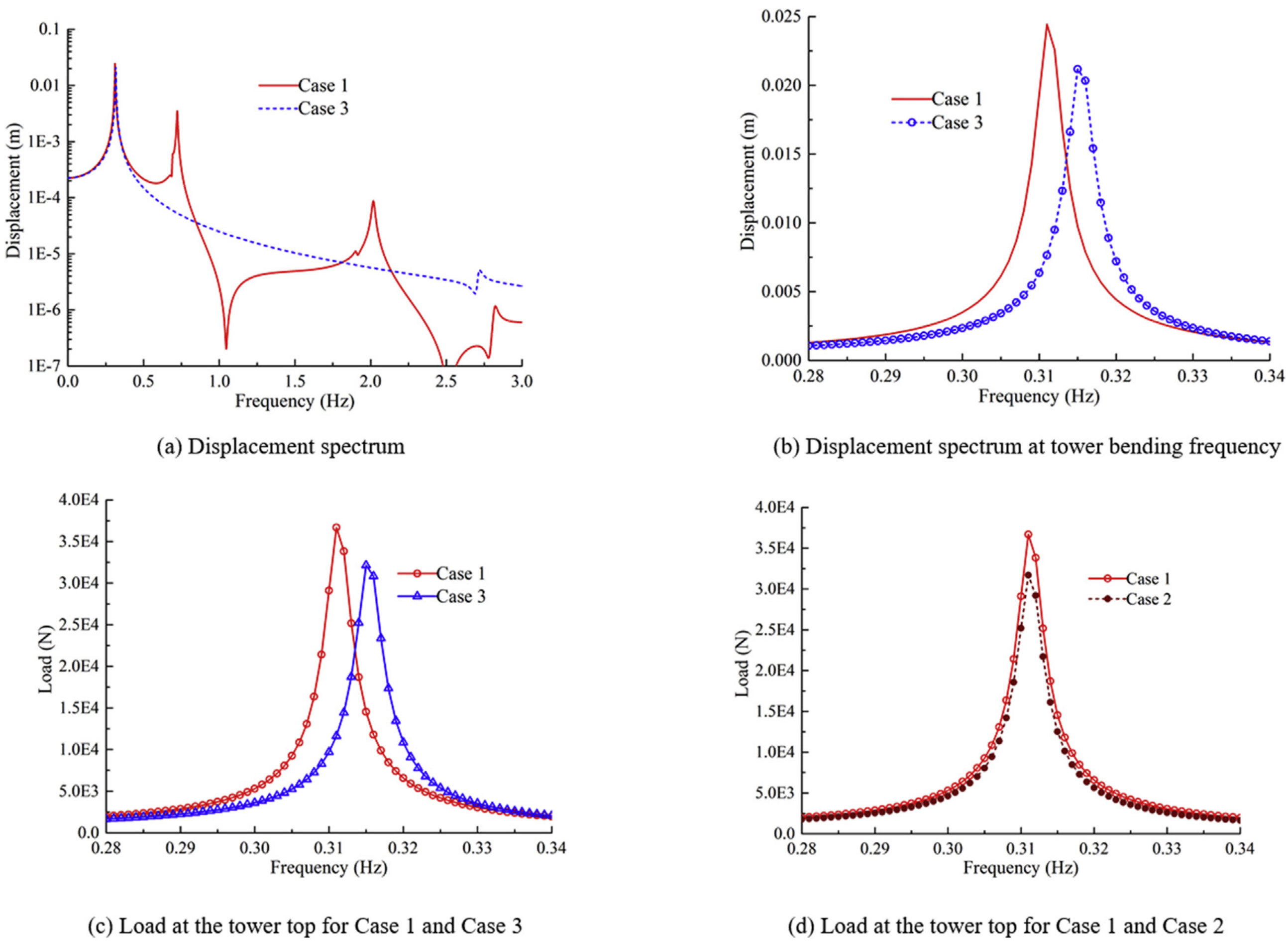

(a) Displacement spectrum

(b) Displacement spectrum at tower bending frequency

(c) Load at the tower top for Case 1 and Case 3

(d) Load at the tower top for Case 1 and Case 2

Fig. 11. Comparison of the frequency domain response of different cases.

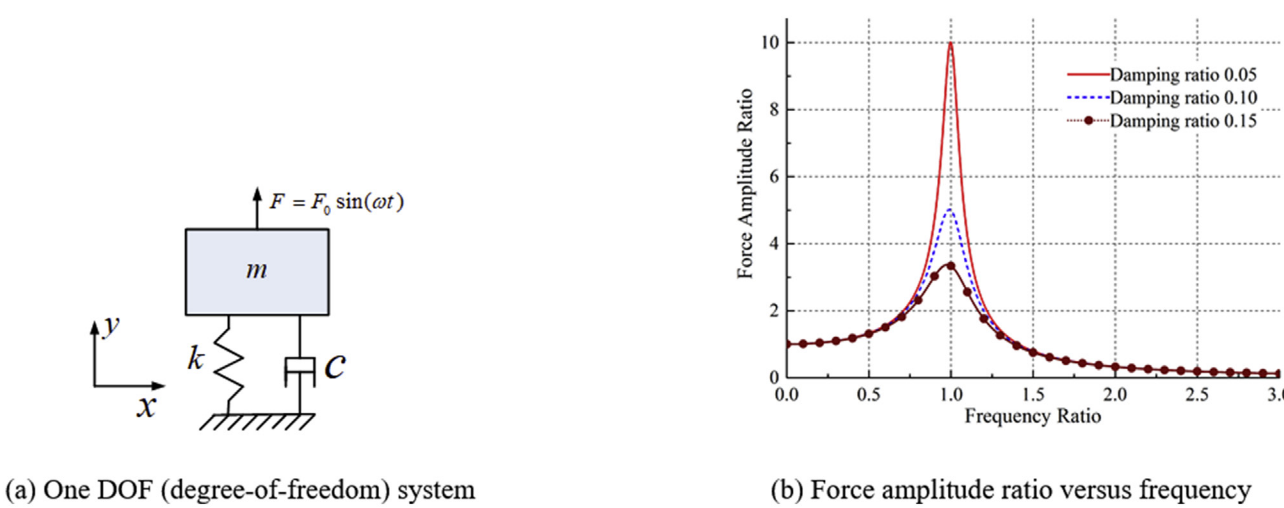

(a) One DOF (degree-of-freedom) system

(b) Force amplitude ratio versus frequency

Fig. 12. Schematic and force amplitude ratio versus frequency of the one DOF system.

$$m\ddot{y} + c\dot{y} + ky = F_0 \sin(\omega t) \tag{24}$$

The base force is

$$F_{\text{sup}} = \sqrt{(ky)^2 + (c\dot{y})^2} \tag{25}$$

So the force amplitude ratio $\overline{F}$ of the base force F_{sup} to the external load F_0 is

$$\overline{F} = \frac{F_{\text{sup}}}{F_0} = \sqrt{\frac{1 + (2\xi\lambda)^2}{(1 - \lambda^2)^2 + (2\xi\lambda)^2}} \tag{26}$$

where ξ is the structural damping ratio. λ is the frequency ratio of the external force frequency to the natural frequency of the structure. Then the plots of the force amplitude ratio $\overline{F}$ versus the frequency ratio λ at different damping ratio ξ are presented in Fig. 12b to show the load transmission along its transmitting route. It is noted that the value of the force amplitude ratio $\overline{F}$ keeps larger than 1.0, or the base force F_{sup} is larger than the external load F_0, until the frequency ratio is over 1.42. As for the blade-tower system, the tower's first-bending frequency is smaller than the blade's first frequency (it means the frequency ratio is smaller than 1.0 when the external load frequency is equal to the tower first-bending frequency). Thus, we may say, the external wind force originally acting on the blade would be amplified (called load amplification effect) as it runs through a flexible body, i.e. running from the top blade to the bottom tower top.

If comparing the tower top displacements of Cases 2 and 3, which have the same wind force loaded at the tower top, or, for this two cases, the load amplification effect owing to the blade flexibility is involved, we can see that the tower displacement gets a little smaller (see Fig. 13a). To have a futher insight into the impact of the elastic deformation of the blade on the tower response, we will observe the mechanical energy consumption, including the kinetic energy and the elastic energy of the blades and the tower, during the dynamic response. The time histories of the mechanical energy distribution of the tower, blade 1 and blade 2 are plotted in Fig. 13b. It is shown that the energy consumed by the tower deformation and vibration is much larger, about 7 times, than that of the blades. Or, the response is mainly dominated by the tower bending motion. Based on the comparison of mechanical energy of the blades and the tower, we can say that, generally, owing to the additional energy consumption caused by the blades the tower displacement gets smaller. But value of this additional energy consumption is much smaller than that of the tower. Therefore the decrease of tower displacement is small.

By now, based on above results of the influences of dynamic and flexible behaviors of top blades on tower response, we may say there are two kinds of influences: on one hand, the wind load running through the flexible blades to the tower may be amplified, and consequently the tower response gets larger up to 15.0% due to the elastic deformation and dynamic motion (called inertial-elastic effect here) of the flexible blade; on the other hand, the tower response drops just a little because the elastic deformation of blade can consume some mechanical energy (called energy-consuming effect), around 10% of the tower. In other words, there is a competition between the energy-consuming effect and inertial-elastic effect of the flexible blade on the overall dynamic response of the wind turbine. For an operating wind turbine, external loads mainly come from the wind forces acting on the rotating rotor/blades. Thus the inertial-elastic effect is the crucial factor that affects the dynamic interaction between tower and blades. In addition to the generally-known design rule that the natural frequency of the structure should be not close to the wind frequency, we note that a larger difference between the natural frequencies of the tower and the blade would be helpful to decrease the tower response, i.e. to decrease the wind load transferring from the blades to the tower top. So, one of our suggestions is to increase the natural frequency of blades, e.g. to use certain material at blade root which has larger values of Young's modulus.

4.2. Coupling mechanism of blade response

4.2.1. Increase of blade displacement caused by elastic tower

For the blade responses, two cases of supporting conditions, i.e. the blades respectively supported on the top of the flexible tower (Case 1 in Fig. 10) and fixed at the root (as a cantilever beam and called Blade 4), are considered here, see Fig. 14. The spectrum curves of blade tip displacement and blade bending energy are presented in Fig. 15. We can see, for Case 1, there is an additional peak at lower frequency (corresponding to the tower first-bending frequency). And the maximum displacement of Blade 1 gets slightly larger, but the displacement peak of Blade 2 gets smaller than Blade 4 (Fig. 15a). It is noted that blade tip displacement is principally caused by two factors, i.e. the tower bending and the blade itself elastic deformation, then the potential energy of Blade 1 (including the two factors) and Blade 4 (including only the factor of blade elastic deformation) are compared in Fig. 15b. It is seen that the elastic deformation and the consequently elastic potential energy of Blade 1 is 16.7% larger than Blade 4 due to the supporting condition of the flexible tower.

If comparing the displacements of the Blade 1 and Blade 2 (of which the supporting conditions are the same but the azimuth angles are different), it is noted that the peak values of the two blades are somewhat different, as shown in Fig. 15a. Because, for the anti-symmetric flapping mode, the two blades actually have different modal displacements as shown in Fig. 16. It means that the blade response is also influenced by its azimuth. Actually, for an integrated wind turbine system, the blades with different azimuth have different modal displacements for a certain mode, so their dynamic responses are somewhat different.

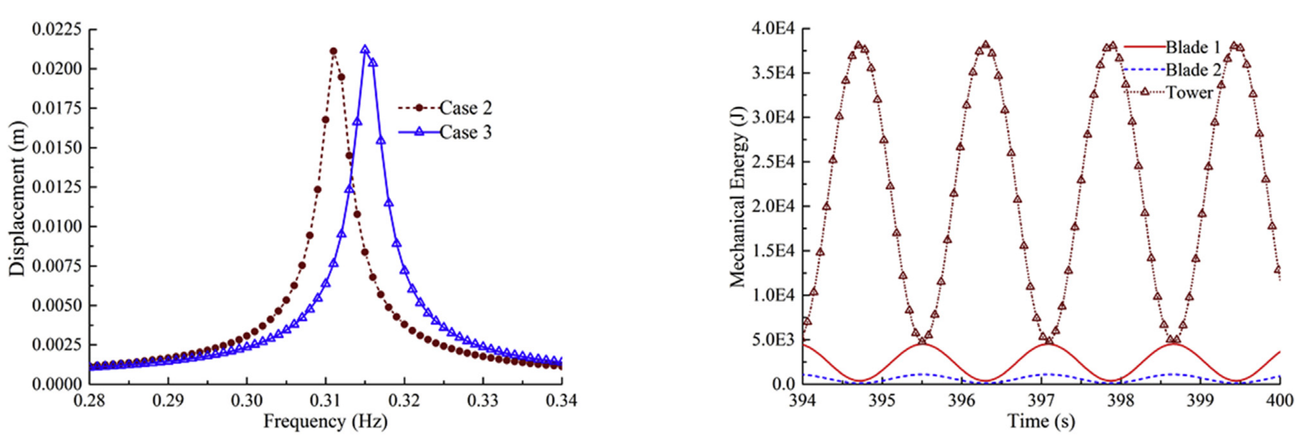

(a) Displacement of tower top for Case 2 and Case 3

(b) Mechanical energy distribution of different parts

Fig. 13. Responses of different parts of the wind turbine.

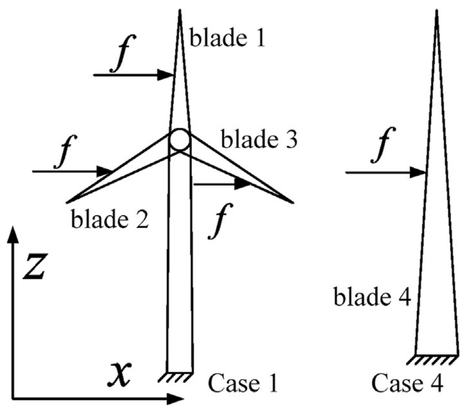

Fig. 14. Two supporting cases of blades (Case1 and Blade 4).

its root by two springs, i.e. a translation spring k_1 and a rotation spring k_2 as shown in Fig. 17, is taken as an example for simplicity and clarity. The governing equation of the elastically supported beam is

$$\rho A\frac{\partial^2 y}{\partial t^2}+EI\frac{\partial^4 y}{\partial x^4}+c\frac{\partial y}{\partial t}=f(x)\sin \omega t \tag{27}$$

Based on the mode superposition method, its steady-state solution can be written as

$$q_n(t)=\frac{f_n}{\sqrt{\left(\omega_n^2-\omega^2\right)^2+\left(2\xi_n\omega_n\omega\right)^2}}\sin(\omega t+\theta) \tag{28}$$

where $q_n(t)$ is the modal displacement of mode $\boldsymbol{n}$, and $\boldsymbol{f_n}$ is the modal force. When $\omega=\omega_n$ (ω_n is the beam natural frequency), Eq.

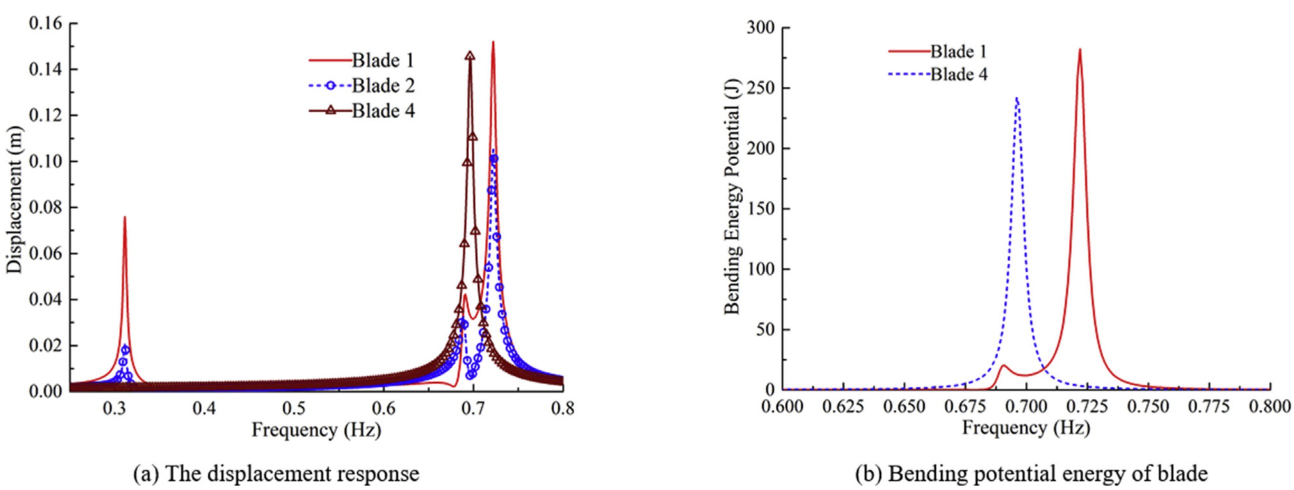

Fig. 15. Displacement and energy response in the frequency domain.

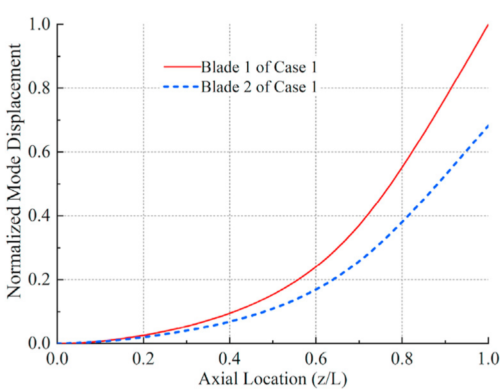

Fig. 16. Normalized model shapes of blades with different azimuths.

4.2.2. Effects of elastic supporting system on blade response

Based on above results we can see that the blade response gets larger because of the bottom flexible tower. Here we would give a further theoretical discussion on this phenomenon and its mechanism. To examine the impacts of base elasticity and base motion on the dynamic response of a blade, a cantilever beam supported at

(28) can be rewritten as

$$q_n(t)=\frac{f_n}{2\xi_n\omega_n^2}\sin(\omega_n t+\theta) \tag{29}$$

Then the particular solution of Eq. (27), i.e. the dynamic response of the beam, is

$$y(x,t)=\frac{f_nX_n(x)}{2\xi_n\omega_n^2}\sin(\omega_n t+\theta) \tag{30}$$

where $X_n(x)$ is the natural modal shape and can be generally expressed as

$$X(x)=a1\cos sx+a2\sin sx+a3\cosh sx+a4\sinh sx \tag{31}$$

And the frequency equation is

$$s^4=\frac{\rho A}{EI}\omega^2 \tag{32}$$

According to the following boundary condition (as shown in Fig. 17)

$$s^4 = \frac{\rho A}{EI}\omega^2$$

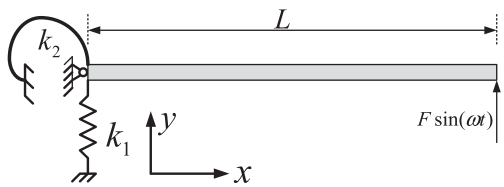

Fig. 17. Schematic of the cantilever beam with flexible supporting base.

$$\begin{array}{ll} Q(0) = EIX'''(0) = -k_1 X(0) & Q(L) = EIX'''(L) = 0 \\ M(0) = EIX''(0) = k_2 X'(0) & M(L) = EIX''(L) = 0 \end{array} \tag{33}$$

and substituting Eq. (31) into Eq. (33) yield

$$\begin{aligned} a1 &= 1 \\ a2 &= \frac{AB(\cos sL - \cosh sL) + 2A(\sinh sL + \sin sL) + (\cos sL + \cosh sL - 2B\sin sL)}{2A(\cosh sL - B\sin sL) + (AB-1)(\sinh sL + \sin sL)} \\ a3 &= \frac{2A(\cos sL - B\sin sL) + (AB+1)(\sinh sL + \sin sL)}{2A(\cosh sL - B\sin sL) + (AB-1)(\sinh sL + \sin sL)} \\ a4 &= \frac{AB(\cos sL - \cosh sL) - (\cos sL + \cosh sL - 2B\sin sL)}{2A(\cosh sL - B\sin sL) + (AB-1)(\sinh sL + \sin sL)} \end{aligned} \tag{34}$$

where $A = EIs^3/k_1$ and $B = EIs/k_2$. Now, we have the dispersion equation as

$$\begin{aligned} &AB(\cos sL\cosh sL - 1) + (A+B)\cosh sL\sin sL \\ &\quad + (A-B)\cos sL\sinh sL - 1 - \cos sL\cosh sL \\ &\quad = 0 \end{aligned} \tag{35}$$

to get the natural frequency of the beam. When the values of the springs' stiffness are infinite, the modal shape, i.e. Eqs. (31) and (34), and the dispersion equation, Eq. (35), will be consistant with the traditional cantilever beam. To compare the responses of the beams respectively with and without elastic supporting base, the displacement distribution along the beam length is given as

$$\overline{A}(x) = \frac{f_n X_n(x)}{\omega_n^2} \tag{36}$$

To study the effects of elastic supporting system on the beam's response, the displacement amplitude distributing along the beam length for two cases of the beam, with different values of rotational stiffness and translational stiffness, are calculated. In one case, the translational stiffness is 8e6N/m and the rotational stiffness varies from 2e7Nm/rads to 8e7Nm/rads; in the other case, the rotational stiffness is 5e7Nm/rads and the translational stiffness varies from 1e7N/m to 8e7N/m. The beam's parameters are listed in Table 4, and the beam natural frequency is 1.452 Hz as its left end is fixed. The natural frequency and displacement amplitude along beam length, with various translational stiffness of the beam, are shown in Fig. 18.

For case of the rotational stiffness changing, see Fig. 18a and c, the displacement amplitude rises and the natural frequency drops

Table 4
Parameters of the cantilever beam.

Parameter	Value	Parameter	Value
Young's Modulus	210 GPa	Length	10 m
Poisson ratio	0.3	Translational stiffness	8e6N/m
Mass density	7800 kg/m^3	Rotational stiffness	8e7Nm/rads
Diameter	0.2 m		

as the rotational stiffness decreases. Or the displacement at free end rises by 8.3%–39.6% because of the elastic supporting base, compared with the beam with a fixed base. For case of the translational stiffness changing, see Fig. 18d, the displacement amplitude at the free end does not change obviously, and the displacement at free end increase by about 14.5% compared with the traditionally fixed beam. So we may say that the elasticity of the supporting base have two effects on the beam, one effect is that it changes the natural frequency, and another effect is that it directly changes the dynamic response. Fig. 18e presents the variation of the beam's maximum displacement against rotational-translational stiffness, where Eq. (36) is used. It is seen that the beam response would increase owing to the base elasticity.

From above discussions we can see that increasing the rotational stiffness of the support system (tower) is a more effective way to reduce the response amplitude of the cantilever beam (blades). So we may say it is recommended to increase the rotating/bending stiffness of tower so that the blade vibration amplitude decreases consequently. And, as we know, the bending stiffness is proportional to the fourth power of its cross-sectional diameter, a proper increase of diameter of the tower root can effectively increase its rotating/bending stiffness. And the increase of tower frequency caused by increasing stiffness can be controlled by adding additional mass.

5. Conclusions

The integrated blade-tower model of a large-sized wind turbine is developed based on finite element simulations so as to carry out dynamic response analysis, in terms of both time history and frequency spectrum, under consideration of tower-balde interactions. Firstly, the dynamic response including the structural displacement and stress of the integrated wind turbine are calculated under random wind loads and compared with the two simplified models. It's found that there mainly are two reasons which are responsible for the response differences, i.e. one is the structural dynamic coupling of flexible bodies and another one is the change of the wind load values at different frequencies.

Secondly, in order to have a deeper insight into the dynamic interaction between the flexible tower and blades, we studied the load transmitting route and mechanical energy distribution through frequency response analysis. The results show that the

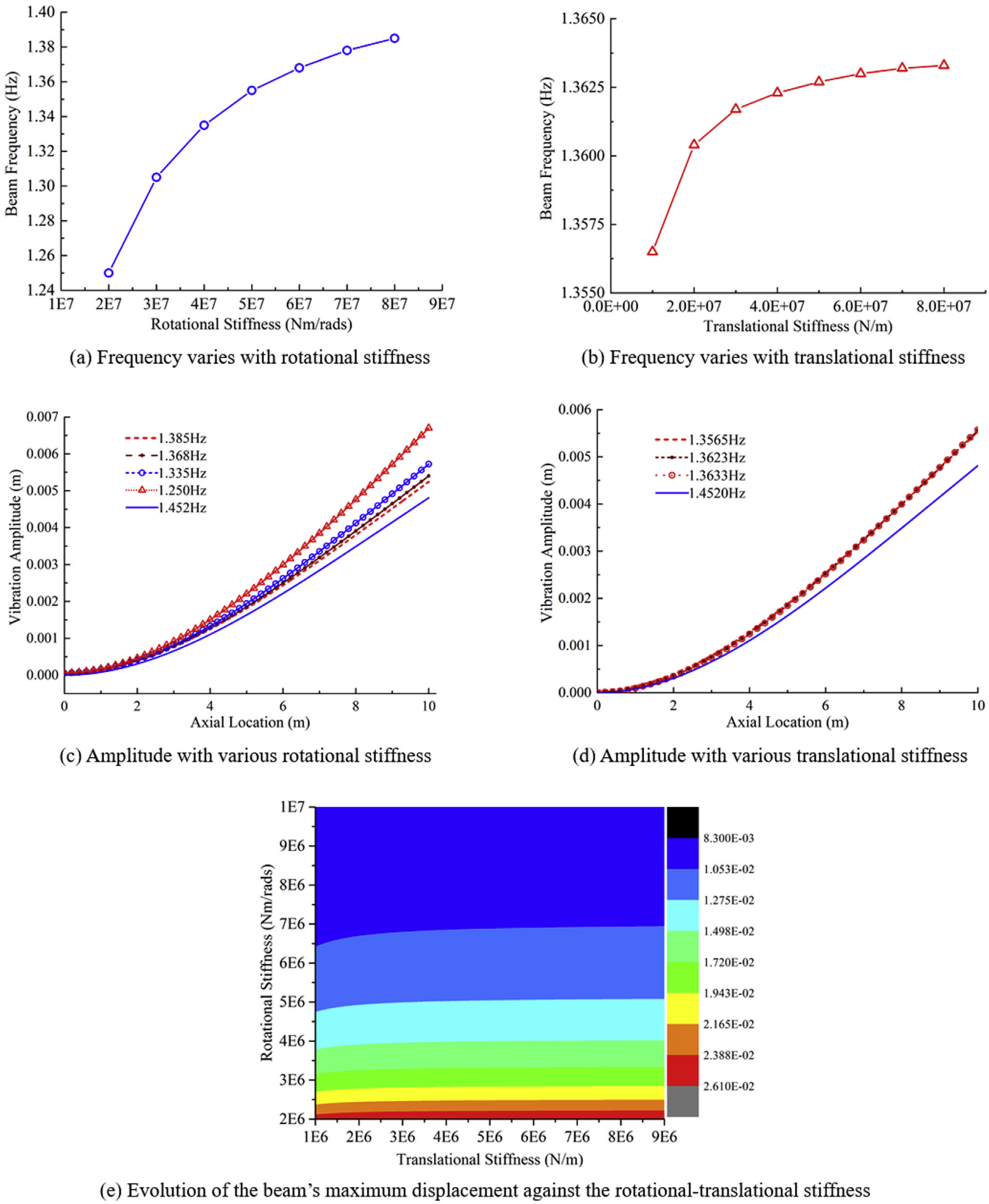

Fig. 18. Beam frequency and displacement amplitude varies with supporting stiffness.

wind load running from the flexible blades to the tower may be amplified, and consequently the tower response gets larger up to 15.0% due to the elastic deformation and dynamic motion (inertial-elastic effect) of the flexible blade; on the other hand, the tower response drops a little because the elastic deformation of blade can consume some mechanical energy (energy-consuming effect), around 10% of the tower. In other words, there is a competition between the energy-consuming effect and inertial-elastic effect of the flexible blade on the overall dynamic response of the wind turbine. In addition to the generally-known design rule that the natural frequency of the structure should be not close to the wind frequency, we note that a larger difference between the natural frequencies of the tower and the blade would be helpful to decrease the tower response, i.e. to decrease the wind load transferring from the blades to the tower top. So, one of our suggestions is to increase the natural frequency of blades, e.g. to use certain material at blade root which has larger values of Young's modulus.

The blade displacement gets up to 22% larger than that without blade-tower interaction. Because the elastic-dynamic behaviors of the tower principally provides a more flexible and vibrating supporting base. Increasing the rotational stiffness of the tower is a more effective way to reduce the response amplitude of the blades. So we may say it is recommended to increase the rotating/bending stiffness of tower so that the blade vibration amplitude decreases consequently. And, as we know, the bending stiffness is proportional to the fourth power of its cross-sectional diameter, a proper increase of diameter of the tower root can effectively increase its rotating/bending stiffness. Additionally, it is noted that the blade displacement actually changes with the blade azimuths, owing to the change of natural modal shape of the integrated wind turbine.

CRediT authorship contribution statement

Shuangxi Guo: Validation, Formal analysis, Visualization, Writing - original draft. **Yilun Li:** Methodology, Computation, Investigation, Writing - original draft. **Weimin Chen:** Concept, Writing - review & editing, Supervision.

Declaration of competing interest

The authors declare that they have no known competing financial interests or personal relationships that could have appeared to influence the work reported in this paper.

Acknowledgments

The authors of this paper would like to thank the financial supports provided by the Strategic Priority Research Programme of CAS (Grant No. XDA22000000) and the National Natural Sciences Foundation (Grant No. 11372320).

References

[1] J. Wang, D. Qin, T.C. Lim, Dynamic analysis of horizontal axis wind turbine by thin-walled beam theory, J. Sound Vib. 329 (17) (2010) 3565–3586.
[2] X. Chen, J. Li, J. Chen, Wind-induced response analysis of a wind turbine tower including the blade-tower coupling effect, J. Zhejiang Univ. - Sci. 10 (11) (2009) 1573–1580.
[3] S. Adhikari, S. Bhattacharya, Dynamic analysis of wind turbine towers on flexible foundations, Shock Vib. (19) (2012) 37–56.
[4] H.M. Negm, K.Y. Maalawi, Structural design optimization of wind turbine towers, Comput. Struct. 74 (6) (2000) 649–666.
[5] N. Bazeos, G.D. Hatzigeorgiou, I.D. Hondros, et al., Static, seismic and stability analyses of a prototype wind turbine steel tower, Eng. Struct. 24 (8) (2002) 1015–1025.
[6] P.J. Murtagh, B. Basu, B.M. Broderick, Along-wind response of a wind turbine tower with blade coupling subjected to rotationally sampled wind loading, Eng. Struct. 27 (8) (2005) 1209–1219.
[7] P.J. Murtagh, A. Ghosh, B. Basu, et al., Passive control of wind turbine vibrations including blade/tower interaction and rotationally sampled turbulence, Wind Energy 11 (2008) 305–317.
[8] A. Spagnoli, L. Montanari, Along-wind simplified analysis of wind turbines through a coupled blade-tower model, Wind Struct. 17 (6) (2013) 589–608.
[9] W.Y. Liu, The vibration analysis of wind turbine blade–cabin–tower coupling system, Eng. Struct. 56 (2013) 954–957.
[10] D. Lee, D.H. Hodges, M.J. Patil, Multi-flexible-body dynamic analysis of horizontal Axis wind turbines, Wind Energy 5 (4) (2002) 281–300.
[11] N. Kang, S. Chul Park, J. Park, et al., Dynamics of flexible tower-blade and rigid nacelle system: dynamic instability due to their interactions in wind turbine, J. Vib. Contr. (2014) 1–11.
[12] Y. Shkara, R. Schelenz, G. Jacobs, The effect of blade-tower interaction on the structure loading of multi megawatt horizontal axis wind turbine, J. Phys. Conf. 1037 (7) (2018), 072033.
[13] H. Kim, S. Lee, S. Lee, Influence of blade-tower interaction in upwind-type horizontal axis wind turbines on aerodynamics, J. Mech. Sci. Technol. 25 (5) (2011) 1351–1360.
[14] Guo SX, Analysis on Dynamic Response of Floating Wind Turbine Considering the Coupling between Elastic Components [D], 2015, Institute of Mechanics CAS. In Chinese.
[15] D.Y. Li, Z.Q. Ye, Y. Chen, Multi-body dynamics numerical analysis of rotating blade of horizontal axis wind turbine, Acta Energiae Solaris Sin. (4) (2005) 473–481. In Chinese.
[16] J.M. Jonkman, S. Butterfield, W. Musial, et al., Definition of a 5-MW Reference Wind Turbine for Offshore System development[M], National Renewable Energy Laboratory Golden, CO, 2009.
[17] C. Lindenburg, Aeroelastic Modelling of the LMH64-5 Blade[M], 2002. Petten.
[18] M.O.L. Hansen, Aerodynamics of Wind Turbines[EB/OL], Taylor and Francis, London, 2013.